Assessing the effects of radiation damage on Ni-base alloys for the prometheus space reactor system

Thomas M. Angeliu [a,*], John T. Ward [a], Jonathan K. Witter [b]

[a] *Lockheed Martin, P.O. Box 1072, Schenectady, NY 12301-1072, United States*
[b] *AREVA NP, Inc., Lynchburg, VA, United States*

Abstract

Ni-base alloys were considered for the Prometheus space reactor pressure vessel with operational parameters of $\sim$900 K for 15 years and fluences up to 1.6×10^{20} n/m^2 ($E > 0.1$ MeV). This paper reviews the effects of irradiation on the behavior of Ni-base alloys and shows that radiation-induced swelling and creep are minor considerations compared to significant embrittlement with neutron exposure. While the mechanism responsible for radiation-induced embrittlement is not fully understood, it is likely a combination of helium embrittlement and solute segregation that can be highly dependent on the alloy composition and exposure conditions. Transmutation calculations show that detrimental helium levels would be expected at the end of life for the inner safety rod vessel (thimble) and possibly the outer pressure vessel, primarily from high energy ($E > 1$ MeV) n, α reactions with ^{58}Ni. Helium from ^{10}B is significant only for the outer vessel due to the proximity of the outer vessel to the BeO control elements. Recommendations for further assessments of the material behavior and methods to minimize the effects of radiation damage through alloy design are provided.
© 2007 Elsevier B.V. All rights reserved.

PACS: 61.82.−d

1. Introduction

Project Prometheus was initiated to develop a space nuclear/electric reactor system for a wide range of deep space and terrestrial missions. The basic concept was a compact fast reactor coupled with a direct gas Brayton cycle turbine that would drive on-board generators for electrical power, Fig. 1. The Jupiter Icy Moon Orbiter (JIMO) mission was selected as the first mission and required operation for up to 15 years. Our involvement was terminated in September of 2005 due to a shift in priorities at NASA. The following is a summary of the efforts to identify a Ni-base alloy for use as the reactor pressure vessel with preliminary design considerations listed in Table 1. From an engineering perspective, a primary concern for this vessel was containing the pressurized helium–xenon coolant/working fluid. From a materials perspective, the primary concerns were thermal creep, corrosion in impure helium, joining and radiation-induced embrittlement. This paper assesses radiation-induced embrittlement relative to the JIMO mission.

* Corresponding author. Tel.: +1 518 395 6163.
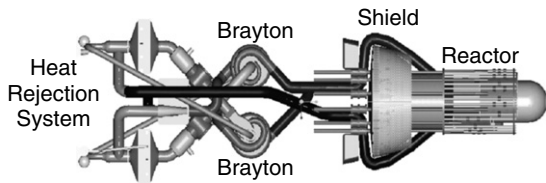 *E-mail address:* angeltm@kapl.gov (T.M. Angeliu).

Fig. 1. Integrated layout of a pre-conceptual Prometheus reactor power system for the Jupiter Icy Moon Orbiter mission.

Table 1
Preliminary considerations for one design of the JIMO pressure vessel

Temperature outer vessel	900 K
Temperature inner vessel (safety rod, thimble)	To be determined (<1050 K)
Temperature hot gas leg	~1150 K
Stress	70 MPa
Ductility	>1%, primarily for lift off, but a concern for ground test unit cycling
Toughness	Needs to be determined
Creep strain	<1% in 15 years
Fluence outer vessel	$<8 \times 10^{25}$ n/m² ($E > 0.1$ MeV)
Fluence inner thimble	$<1.6 \times 10^{26}$ n/m² ($E > 0.1$ MeV)
Environment	Outer diameter: space vacuum Inner diameter: He/Xe with impurities
Other	Mass (~8 mm thick wall), Neutronics

Ni-base and refractory metal alloys were considered for the pressure vessel as conventional austenitic and ferritic/martensitic steels do not have sufficient thermal creep resistance to meet the design criteria of less than 1% strain at 900 K/70 MPa for 130 000 h. Design trade studies favored Ni-base alloys for two main reasons, both related to a primary engineering concern over a single point failure in the pressurized working fluid loop that would end the mission. First, refractory metal alloys are susceptible to radiation-induced hardening and embrittlement at temperatures below ~0.3 of the melting point or 800–1100 K. Secondly, fabrication of a dissimilar metal joint between a refractory metal alloy and a conventional alloy plant component would be very challenging due to the propensity for a reduction in the joint ductility due to intermetallic formation. Due to these concerns, one preliminary design recommended the use of a Ni-base alloy pressure vessel, eliminating the dissimilar metal joint concern. However, many studies have shown that Ni-base alloys are also compromised by radiation-induced damage. From 1974 to 1985, Ni-base alloys

were investigated for advanced cladding and duct materials for the United States Liquid Metal Fast Breeder Reactor (LMFBR) [1]. Ni-base alloys were selected on the basis of their swelling resistance, sodium compatibility and high temperature thermal creep strength, coupled with an extensive industrial base for processing, fabrication and joining [2,3]. Early experiments revealed that Ni-base alloys with greater than about 40% Ni had excellent swelling resistance [4]. However, these materials were susceptible to radiation-induced grain boundary embrittlement. Several embrittlement mechanisms were proposed, including differential strengthening with radiation-induced precipitation of grain boundary phases [5] and the formation of He bubbles on grain boundaries [6]. Due to this embrittlement, Ni-base alloys were abandoned in favor of swelling and embrittlement resistant austenitic and ferritic/martensitic steels [7]. More recently, Ni-base alloys were investigated for fusion reactors as the first wall material. Initial studies revealed that the relatively high levels of neutron damage (>100 displacements per atom (dpa), $>2 \times 10^{27}$ n/m², $E > 0.1$ MeV) would result in significant helium generation [8], so other materials were pursued.

For the JIMO mission, the expected neutron fluences would have been generally lower than those investigated in the LMFBR and significantly lower than the fusion studies, with a maximum fluence of $\sim 1.6 \times 10^{26}$ n/m² (8 dpa), $E > 0.1$ MeV, for the thimble region and $\sim 8 \times 10^{25}$ n/m² (4 dpa) for the pressure vessel. Cross sections showing details of the one pre-conceptual core geometry are shown in Fig. 2. Encouragement for using Ni-base alloys was provided by the successful use of Nimonic PE16 as fuel cladding for the Dounreay prototype fast reactor (PFR) in the UK [9]. This material experienced $>1.6 \times 10^{27}$ n/m² (80 dpa) without a single failure at 673–998 K, showing that designs are possible despite the well documented radiation-induced embrittlement. In addition to the precipitation strengthened PE16, solid solution strengthened Ni-base alloys Hastelloy X, Alloy 617 and Alloy 230 were considered as vessel materials, Table 2. Ni-base materials highly alloyed with Al and Ti, and thus cast alloys, were not considered despite their superior creep strength due to limited weldability. Solid solution strengthened Alloys 617 and 230 are more recently developed than Hastelloy X and exhibit superior phase stability and mechanical properties, such as creep strength [10,11]. There are very limited neutron irradiation data for solid solution strength-
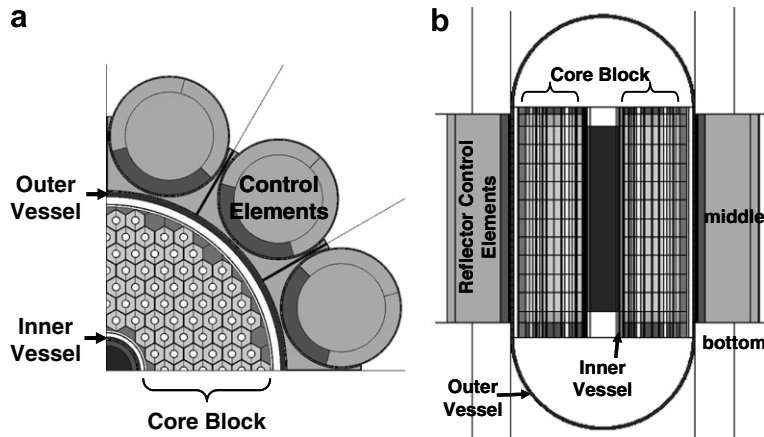
Fig. 2. Details from a schematic cross section of a pre-conceptual Prometheus reactor core geometry for the Jupiter Icy Moon Orbiter mission: (a) top view; and (b) side view.

Table 2
The composition of commercial alloys considered for the JIMO pressure vessel and recommended compositions for nuclear grade versions (wt%)

Alloy	Ni	Cr	Fe	Mo	W	Co	Ti	Al	Mn	C	Other
Alloy 617	54	22	–	9	–	12.5	0.3	1.0	–	0.07	
617NG	54	22	–	9	–	12.5	0.3	0.8	0.3	0.08	<1 wppm B
617L	54	22	–	9	–	12.5	–	–	0.3	0.08	<1 wppm B
Alloy 230	57	22	<3	2	14	<5	–	0.3	0.5	0.10	0.4Si, 0.02La, <0.015B
230NG	61	22	–	2	14	0.5	–	0.2	0.3	0.10	<1 wppm B
230L	61	22	–	2	14	0.5	–	–	0.3	0.10	<1 wppm B
Nimonic PE16	44	17	33	3.7	–	–	1.2	1.3		0.05	
PE16NG	44	17	33	3.7	–	–	1.2	1.3	–	0.05	<1 wppm B
Hastelloy X	47	22	18.5	9	0.6	1.5	–	–	0.5	0.10	0.5Si, <0.008B
Haynes 188	22	22			14	39					

L, L-grade; NG, nuclear grade.

ened Ni-base alloys, none for Alloys 617 and 230 and little for Hastelloy X. The following sections summarize the effects of neutron irradiation on the swelling, creep and mechanical behavior of relevant Ni-base alloys. A summary of the literature reviewed is found in Table 3. This review was not meant to be comprehensive, but illustrative of the major behaviors reported. A more comprehensive review of these effects on austenitic materials can be found in Ref. [12]. In general, experimental data were lacking to address design considerations and extensive radiation test programs were required.

2. Radiation-induced swelling

The United States National Cladding/Duct Materials Development Program was initiated for the development of reference and advanced materials for liquid metal fast breeder reactor applications.

Initial experiments included the screening of many commercial alloys for radiation-induced swelling. In the first experiment, B-109, thirteen alloys were exposed to a fast spectrum at the Experimental Breeder Reactor-II (EBR-II). A second experiment (AA-1) narrowed this evaluation to six alloys. In these experiments, materials were irradiated to fluences of 1.2–1.5×10^{27} n/m^2 ($E > 0.1$ MeV) at temperatures from 673 K to 923 K. A minimum in the swelling behavior was reported at Ni contents between 40 and 50 wt%, with PE16 displaying some of the lowest swelling behavior [4]. These initial studies also showed that aging treatments applied to both solution annealed and cold worked alloys increased swelling, but the reason was not fully understood. Additional swelling studies with PE16 in EBR-II produced less than 1% swelling after irradiation between 44 and 77 dpa (8.8×10^{26}–1.5×10^{27} n/m^2) at 667–909 K [6]. Lower swelling

Table 3
A literature summary on the effects of neutron irradiation on Ni-base alloys

Alloy	Fluence (n/m^2)	Irradiation T (K)	Test T (K)	Property	Comments	Reference
PE16	$<1.5 \times 10^{27}$	673–923		Swelling	Minimum at 40–50 wt% Ni	[4]
PE16	44–74 dpa[a]	667–909		Swelling	<1% Swelling	[6]
PE16		300–1073	300–1073	Swelling	He implantation	[55]
PE16	<280 dpa[a]	798		Swelling	<1%, used C ion bombardment	[57]
PE16	$<9 \times 10^{26}$	673–873		Swelling	29 wppm B had less swelling than 50 wppm B	[13,14]
PE16	8 dpa[a]	503–623	923	Creep		[19]
PE16	5 dpa[a]	823,858	823,858	Creep		[19]
PE16	1.5×10^{23}[b] to 7×10^{22}	318	923	Creep	Reduction in creep rupture, ductility and rupture time	[23]
PE16	7.8×10^{25}	693–785	693–785	Creep	Creep-in-bending, in situ	[18]
PE16	2 to 17×10^{26}	813	813	Creep	Pressurized tubes	[17]
PE16	5×10^{26}	773–1000	773–1000	Tensile	Strain rate effect	[43]
PE16	<50dpa	503–623	<973	Tensile	Very low elongations at 973 K	[19]
PE16	<20 dpa	823, 953	823, 953	Tensile	Low elongations	[19]
PE16			673–923	Tensile	Implanted with He and Li	[25]
PE16	2×10^{24}	318, 923	973	Tensile	Low ductility	[58]
PE16	$1.2–4.0 \times 10^{26}$	650–823	683–973	Tensile	Effect of heat treat, includes swelling effects	[38]
PE16	2 to 5×10^{26}	723–898	698–1008	Tensile	Ductility decrease attributed to γ' on grain boundaries	[39]
PE16	$2,5,7 \times 10^{26}$	400–1008	823–973	Tensile	Ductility trough of near zero ductility after irrad.	[5]
PE16	20–29 dpa	748,823, 923	748,823, 923	Tensile	Low B increases ductility from 0.1% to 1.5 to 2.0%	[19]
PE16	5.7×10^{26}	738–850	783–933	Ring test	Much reduced ductility, lowest at 823 K	[56]
Hast X	5×10^{26}	873–923	873–923	Swelling	Relates swelling to precipitate microstructure	[15]
Hast X	[b]	923	923	Creep	Decreased rupture strength	[22]
Hast X		889–944	889–944	Creep	No fluence reported	[20]
Hast X	6.6×10^{24}[b]		1173	Creep	Radiation increased creep strength	[33]
Hast X	1.1×10^{26}	923	823–1123	Tensile	Elongations <1%, No change in yield, strain rate effect	[44]
Hast X	3.3×10^{24}	811	856, 977	Tensile	Includes alloys 625, 800	[28]
Hast X	3.3×10^{24}	299, 866, 977	300	Tensile	Reduced ductility at all T, hardening at 299 K & 866 K	[22]
Hast X	1.1×10^{25}[b]	648	873–1123	Tensile	Good ductility at elevated temperature testing	[22]
Hast X	$10^{24}–10^{25}$[b]		873–1273	Tensile	Low B (<0.2 wppm) retains high ductility (28%)	[22]
Hast X	$<2 \times 10^{25}$[b]		1173, 1273	Tensile	~10X reduction in tensile ductility	[32,33]

[a] 1 dpa is $\approx 2 \times 10^{25}$ n/m^2 for Ni-based alloys [13].
[b] Denotes thermal neutrons, otherwise all fluences were fast.

was also reported for PE16 containing 25 wppm B, rather than 50 wppm B, after irradiation in the Dounreay fast reactor up to 9×10^{26} n/m² (48 dpa) between 673 and 873 K [13,14]. Based on these results, it can be expected that PE16 would exhibit acceptable swelling behavior for the JIMO vessel application.

Swelling studies on solid solution strengthened Ni-base alloys focused on Alloy 625, Hastelloy X and Alloy 800. These materials produced <0.6%, 0.6–2.1% and 0.5–5% swelling respectively after exposure in EBR-II to 5×10^{26} n/m² at 873–923 K [15]. The variation in the swelling behavior was attributed to the precipitate microstructure. The Ni-base Alloy 800 has no second phase strengtheners and swells similar to 304SS. Alloy 625 has much finer, semi-coherent γ'' precipitates that are believed to lower the overall point defect concentration by providing sites for annihilation of vacancies and interstitials. Likewise, the swelling resistance of PE16 has been attributed to the presence of fine, coherent precipitates of γ'. This analysis suggests that more swelling can be expected in Hastelloy X than PE16, but the values should be less than one percent for the JIMO mission. It is more difficult to predict the amount of swelling for Alloys 617 and 230 since no radiation data have been found. Alloy 617 contains sufficient aluminum to form γ' and could be expected to behave like PE16 since the aluminum contents are similar. Alloy 230 precipitates a homogeneous distribution of carbides during thermal exposure, which may produce swelling behavior similar to Hastelloy X. The EBR-II study demonstrated adequate swelling resistance for Hastelloy X (0.6–2.1%) at 5×10^{26} n/m² and at temperatures relevant to JIMO. This suggests that at mission fluences up to 1.60×10^{26} n/m², the related alloys of 617 and 230 may have adequate swelling resistance. However, swelling data must be obtained to determine upper limits relative to fluence before committing these materials to an actual design. For example, very poor swelling behavior was reported for Hastelloy X when irradiated at 114 dpa, or 10 times the expected JIMO fluence [16].

3. Irradiation-induced creep

Studies to characterize the irradiation-induced creep behavior of Ni-base alloys are very limited, with more work being reported for post-irradiation experiments than in-pile. Biaxial creep specimens of PE16 were irradiated at ≈813 K at fluences of 2 and 4×10^{26} n/m² ($E > 0.1$ MeV) in EBR-II [17]. Four pressurized tubes of each PE16 heat treat condition were studied, one at zero stress and the others at the three stresses of 55, 110 and 170 MPa. These results showed that the total strain in the solution annealed condition did not exceed 0.4% at the highest stress of 170 MPa (24.7 ksi). This strain was a combination of irradiation creep, thermal creep and swelling, thus the irradiation creep component was no more than 0.4%. An irradiation creep in-bending experiment was conducted for solution annealed and aged PE16 in EBR-II. Minimal creep strain was reported after exposures of 4.8×10^{25} n/m² at 755 K (0.03% creep strain) and 7.2×10^{25} n/m² at 693 K (0.11%) [18]. From these limited data, minimal amounts of irradiation-induced creep were expected. Much more additional data were required, especially on the solid solution strengthened Ni-base alloys where no data were found.

4. Post-irradiation creep

The post-irradiation tensile creep of PE16 was conducted after two different irradiation conditions at the Dounreay fast reactor [19]. In one condition, PE16 was irradiated to 1.6×10^{26} n/m² (8 dpa) at 503–623 K and then thermally crept at 923 K. These specimens exhibited an increase in the secondary creep rate in the solution annealed and aged conditions relative to unirradiated materials. In another post-irradiation creep experiment, PE16 was irradiated at a lower fluence (5 dpa, 1×10^{26} n/m²) and higher temperatures (823 K and 858 K) and then crept at the irradiation temperatures. These experiments showed a reduction in the secondary creep rate and increases in the creep rupture strength for the irradiated material. Although the results from these studies are mixed, none of these results show that radiation significantly influenced the creep behavior for the reported conditions. In-pile creep data are far superior to post-irradiation data as in-pile results are much more representative of service conditions.

Hastelloy X was also evaluated using biaxial stress-rupture specimens as part of a fuel cladding evaluation for a space power reactor, Irradiation Experiment NAS-120 [20]. Unirradiated and irradiated specimens were crept at 922 K and 977 K. All of the irradiated specimens ruptured in less than about 600 h, even at the lowest stress levels of 132 MPa at 922 K and 101 MPa at 977 K. Unfortunately, no creep strain data or irradiation

conditions were reported. The most significant result was that the irradiated creep rupture ductility was less than 2.1%. Unirradiated creep rupture data were not reported, but creep rupture strain for Hastelloy X can exceed 40% at 1033 K and 100 MPa [21]. In another experiment, post-irradiation creep studies on Hastelloy X reported a decrease in the stress rupture strength after thermal neutron irradiation to 5×10^{23} n/m^2 at 923 K [22]. Little difference in the minimum creep rate of Hastelloy X was reported after exposure to neutron irradiation at 889–944 K in excess of 13 000 h in the Hanford Reactor [20]. As with PE16, these limited data suggest that radiation does not significantly influence the creep strain, however, the creep rupture ductility was significantly reduced.

5. Radiation-induced embrittlement

The radiation-induced embrittlement of Ni-base alloys is well known, but quantification based on time, temperature, energy spectrum, flux and composition are lacking [23,24]. At very high temperatures $(T > 0.5 T_{\mathrm{m}})$, embrittlement has been attributed primarily to the formation of grain boundary helium gas bubbles [8]. At lower temperatures $(0.3–0.6 T_{\mathrm{m}})$, helium, radiation-induced solute segregation and precipitation are believed to contribute to embrittlement [24]. Helium is primarily produced in Ni-base alloys by high energy (fast) neutron reactions with Fe, Cr and Ni isotopes and two reactions that occur throughout the neutron energy spectrum. Natural Ni contains 68% ^{58}Ni and 26% ^{60}Ni, with the fast neutron n, α reactions of

$$^{58}\mathrm{Ni} + n_{\mathrm{f}} \rightarrow {}^{55}\mathrm{Fe} + {}^{4}\mathrm{He}, \tag{1}$$

$$^{60}\mathrm{Ni} + n_{\mathrm{f}} \rightarrow {}^{57}\mathrm{Fe} + {}^{4}\mathrm{He}. \tag{2}$$

The high thermal neutron cross section of ^{10}B, which makes up $\sim$20% of naturally occurring boron, is responsible for significant transmutation at relatively low thermal fluences by the n, α reaction of

$$^{10}\mathrm{B} + n \rightarrow {}^{7}\mathrm{Li} + {}^{4}\mathrm{He}. \tag{3}$$

Systematic experimental studies have shown that Li can also contribute to a loss in ductility, but helium was reported to be a more effective embrittling agent [25]. This is consistent with atomistic modeling results [26,27]. Helium can also be produced by the two step reaction of

$$^{58}\mathrm{Ni} + n \rightarrow {}^{59}\mathrm{Ni} + \gamma, \quad {}^{59}\mathrm{Ni} + n \rightarrow {}^{56}\mathrm{Fe} + {}^{4}\mathrm{He}, \tag{4}$$
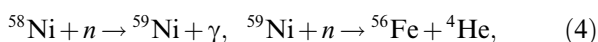
but this reaction requires production of ^{59}Ni first. Helium generation is very dependent on the energy spectrum, cross section and fluence and has been reported as atomic parts per million (appm) versus fluence for a variety of fast, thermal and mixed spectrums [8,28–32]. For Ni-base alloys, it has been reported for a thermal neutron dominant reactor that the transmutation of boron to helium dominates at low fluences (to about 10^{24} n/m^2), while helium from Ni–neutron interactions dominates at high fluences (above 10^{24} n/m^2) [33]. For a fast reactor environment relevant to the Dounreay prototype fast reactor, the helium production rate was reported to be $\sim$1 appm per dpa for materials exposed up to $\sim$100 dpa [34]. Note that 1 dpa is $\sim$2 $\times 10^{25}$ n/m^2 [13]. This trend was based on linear estimates for greater than 40 dpa exposures and may not account for low fluence effects depending on the amount of thermal neutrons and ^{10}B [32,35]. Calculations at energy spectrums typical of the JIMO design and at lower fluences are provided in the following section.

Mechanistically, helium is believed to embrittle grain boundaries by the stress enhanced growth of voids by reducing the energy for the nucleation and growth of these grain boundary voids [8]. While this mechanism has been supported by many studies, there are still unanswered questions about the sensitivity of bubble nucleation and growth with materials and exposure parameters. Very limited work has been reported to correlate the mechanical properties to helium generation. One study on Hastelloy X reported a progressive decrease in the total elongation as a function of thermal neutron dose and calculated amount of helium, Table 4, although no microstructural characterization was reported [32]. In general, no predictions of the mechanical properties are yet possible for a given material with a given set of experimental parameters. This situation is further complicated by the complex effects of radiation-induced solute segregation and grain boundary precipitation.

Radiation-induced solute segregation is a non-equilibrium segregation process that occurs at point defect sinks during irradiation at $\approx$0.3–0.5 of the melting point [36]. Radiation produces point defects in excess of thermal equilibrium concentrations. At high temperatures, these defects are mobile and travel to low energy sites such as grain boundaries, and can interact with solute elements along the way to promote enrichment or depletion at grain boundaries. If the enrichment exceeds the solubility limit,

Table 4
The effect of thermal neutron dose on the total elongation of Hastelloy X tensile tested at 0.67% strain/min ($\sim 1.1 \times 10^{-4}$ s^{-1}) [32]

T_{test} (K)	Thermal neutron dose (n/m^2)	Calculated helium (appm)	Total elongation (%)
973	NA	0.04	30
	NA	0.4	20
	NA	4	8
1173	2.7×10^{21}	0.004	50
	2.2×10^{22}	0.04	40
	2.4×10^{23}	0.4	20
	4.3×10^{24}	5	7
	2.0×10^{25}	40	5
1273	2.7×10^{21}	0.004	40
	2.2×10^{22}	0.04	30
	2.4×10^{23}	0.4	6
	4.3×10^{24}	5	4

second phases may form. The segregation of impurity elements such as S, P, Sb, As, Sn, etc. are well known to embrittle grain boundaries, especially for steels where increases in the hardness along with impurity segregation act synergistically to lower ductility [37]. Auger analysis of PE16 grain boundaries irradiated in EBR-II revealed slight enrichments of P and S, a release of helium upon fracture, changes in the bulk alloying elements and a continuous layer of γ′ along the grain boundaries [38,39]. In general, the literature indicates that radiation-induced solute segregation promotes a continuous grain boundary coverage of intermetallic phases that are more detrimental to radiation-induced embrittlement than segregated impurities such as S and P.

Mechanistically, continuous grain boundary coverage by intermetallics promotes embrittlement by restricting grain boundary deformation, especially when the matrix becomes hardened [4]. Without sufficient plasticity to accommodate strain, these factors act to promote grain boundary failure at relatively lower levels of plastic strain. It is well documented that a continuous layer of γ′ can form along the grain boundaries of irradiated, precipitation hardened Ni-base alloys, including solution annealed PE16 and has been associated with significant decreases in ductility [4,39–41]. For aged PE16, the coverage of γ′ on grain boundaries after irradiation is expected to be less pronounced than for solution annealed material and contribute less to embrittlement [6]. Wrought solid-solution strengthened Ni-base alloys that contain little to

no elements that form intermetallics (Ti, Nb and Al) are believed to be less susceptible to this embrittlement. All of the Ni-base alloys considered for JIMO (PE16, Alloy 617 and Alloy 230) contain the intermetallic former Al while PE16 and Alloy 617 contain Ti and may be susceptible to radiation-induced precipitation on grain boundaries. Correlations between the Al or Ti contents and embrittling exposure conditions have not been established, so compositional limits cannot be recommended.

5.1. Review of mechanical test data

There has been a significant amount of mechanical testing conducted on irradiated Nimonic PE16 and a lesser amount on other Ni-base alloys of interest, Table 3. The data consistently show that irradiation increases the yield and ultimate tensile strengths with a corresponding decrease in tensile ductility. Only two illustrative studies for PE16 are presented. In the first example, the tensile and yield strengths were determined for PE16 irradiated at two conditions in the Dounreay fast reactor [19]. In one condition, PE16 was irradiated to 20 dpa (4×10^{26} n/m^2) at 503–623 K and then tested from 573 K to 1023 K. In another irradiated condition, PE16 was irradiated and tested at 823 K and 858 K. After both exposures, PE16 showed radiation hardening with increased yield strengths, especially at the lower tensile test temperatures. Fig. 3 shows the significant increase in the yield strength and decrease in total elongation at 823 K and 873 K.

In the second example, solution annealed (not aged) PE16 was irradiated in EBR-II at fluences of 1.8, 4.3 and 7.1×10^{26} n/m^2 at temperatures ranging from 723 K to 1008 K [5]. Tensile specimens were tested at 400 K, representing refueling temperatures, the irradiation temperature and 110 K above the irradiation temperature, representative of a temperature excursion. Tensile testing at 400 K showed significant strengthening after irradiation, but the ductility still exceeded 10% elongation. Tensile testing at the irradiation temperature showed significant increases in the yield strength for test temperatures below 923 K with minimal increases in the tensile strength. The ductility of these specimens decreased significantly, as low as 1.5% at 833 K, Fig. 4(a). When specimens exposed to these same conditions were tensile tested at 110 K above the irradiation temperature, the ductility was
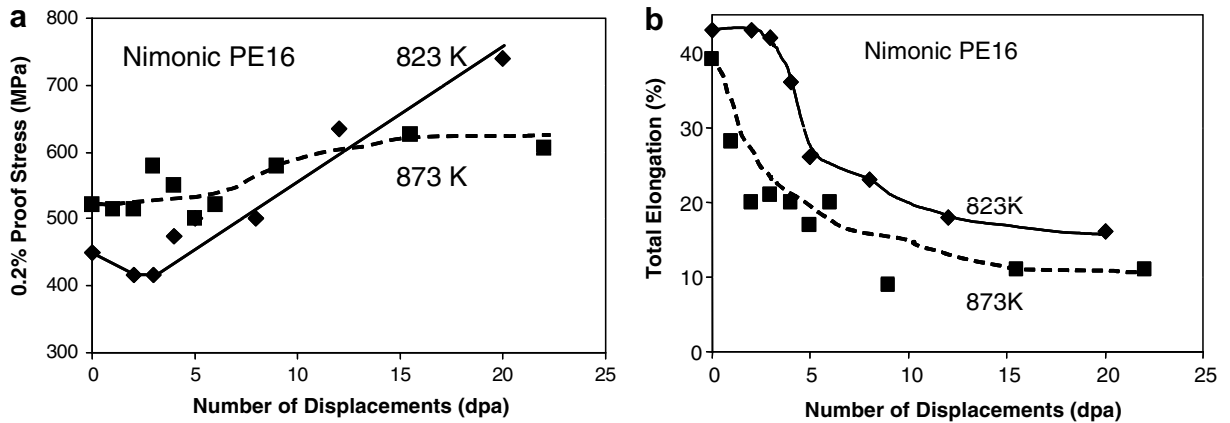
Fig. 3. The dependence on damage level of the tensile properties of Nimonic PE16 (heat treatment 3) irradiated and tested at 823 K to 873 K [19]: (a) yield strength; and (b) total elongation.

reduced even further and in some cases, near zero ductility was observed, Fig. 4(b). These results were attributed to differential strengthening, or the large difference in the strength of the matrix to that of the grain boundary, resulting in intergranular fracture. In this mechanism, irradiation increases the strength of the matrix to a point where deformation primarily occurs at grain boundaries, resulting in low ductility. The authors argued against grain boundary weakening mechanisms such as helium embrittlement and solute segregation, but no direct evidence was provided showing that these mechanisms were not operating. Data used to advocate that helium embrittlement was not applicable were found to be statistically insignificant [42].

For solid solution strengthened Ni-base alloys, the effects of neutron irradiation on the mechanical properties are similar to those reported for precipi-

tation hardened alloys. The yield and ultimate tensile stresses are increased and the elongation to failure is decreased. Tables 4 and 5 show significant decreases in the tensile ductility of Hastelloy X with thermal and fast neutron exposure, respectively [32,28]. The fast neutron exposed materials exhibited brittle grain boundary failure while the unirradiated specimens displayed ductile transgranular failure. No microstructural characterization was conducted to assess the effects of radiation-induced segregation and precipitation, although thermal aging did decrease the ductility, Table 5.

The strain rate is important to the mechanical behavior of irradiated Ni-base alloys as the loss in ductility is more pronounced as the strain rate decreases and the temperature increases. For solution annealed and aged PE16 irradiated to $\sim 5 \times 10^{26}$ n/m^2 in EBR-II, a decrease in the strain
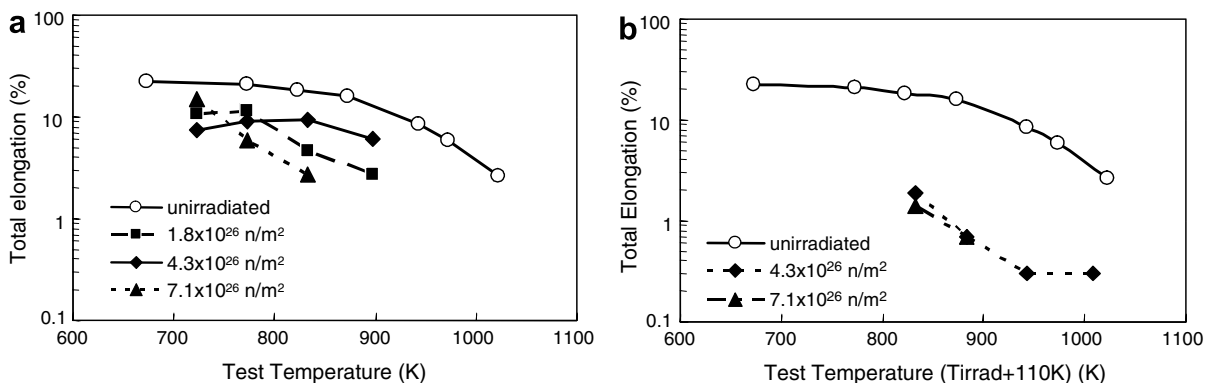

Fig. 4. A significant decrease in the total elongation of Nimonic PE16 when tested at (a) the irradiation temperature (T_{irrad}); and (b) 110 K above T_{irrad} [5]. (a) Tested at T_{irrad}; and (b) tested at 110 K above T_{irrad}.

Table 5
The effect of fast neutron irradiation on the tensile properties of Hastelloy X before and after exposure in EBR-II at/or aged at 856 K for 200 h [28]

T_{test} (K)	Fast neutron exposure (n/m^2)	Yield stress (MPa)	UTS (MPa)	Uniform elongation (%)	Total elongation (%)
299	None	300	863	50	54
	None-aged	308	724	44	47
	3.3×10^{24}	450	945	16	16
856	None	183	661	55	57
	None-aged	223	609	44	46
	3.3×10^{24}	361	709	14	15
977	None	184	425	41	50
	None-aged	181	414	26	35
	3.3×10^{24}	333	427	5.4	8.4

rate by two orders of magnitude reduced the total elongation up to a factor of 10, Table 6 [43]. For Hastelloy X irradiated to 1.1×10^{26} n/m^2 in a mixed spectrum reactor (BR 2 in Belgium), the loss in ductility was more severe as the test strain rate decreased and the temperature increased, Table 7 [44]. Unfortunately, no unirradiated materials were tested for comparison, so it is difficult to assess how much of this behavior is attributed to irradiation and how much to creep. One study on Hastelloy X showed similar decreases in ductility as a function of strain rate for irradiated and unirradi-

ated material [32]. If helium were enhancing grain boundary voiding, then slower strain rates would allow more time for helium diffusion and creep damage to accumulate at grain boundaries to produce intergranular fracture morphology. Very limited creep rupture data for irradiated Hastelloy X illustrate the extent of creep rupture ductility loss, but no comparison was made to unirradiated, thermally aged material to determine if this effect was due to irradiation or thermal aging [20]. Experiments and modeling of PE16 indicate that low failure strains are a result of closely spaced cavities at grain boundary helium bubbles [34]. At low stresses, the rupture life of irradiated Ni-base alloys may be determined by the rate of gas-driven bubble growth rather than by their unirradiated creep strength.

6. Predicted helium generation and embrittlement of the JIMO reactor vessel

Based on prior studies, radiation-induced embrittlement appears to be a major concern, but critical parameters such as fluence, temperature, composition and ductility vs. appm He are not well understood. To better understand the susceptibility to helium embrittlement, transmutation calculations were conducted to determine the amount of helium produced in the candidate pressure vessel material Alloy 617 as a function of the exposure time for

Table 6
The effect of tensile strain rate on the ductility of neutron irradiated PE16 (solution annealed and aged) tested at T_{irrad} + 110 K [43]

Specimen No.	T_{irrad} (K)	T_{test} (K)	Strain rate (s^{-1})	Yield (MPa)	UTS (MPa)	% Uniform elongation	% Total elongation
H12	773	883	4×10^{-2}	717	830	5.5	5.5
H29	773	883	4×10^{-4}	749	770	0.7	0.7
H37	833	943	4×10^{-2}	634	726	3.5	3.5
H42	833	943	4×10^{-4}	644	652	0.3	0.3
H103	898	1008	4×10^{-2}	661	867	3.3	3.3
H111	898	1008	4×10^{-4}	527	534	0.3	0.3

Table 7
The effect of tensile strain rate on the ductility of Hastelloy X irradiated to 2.0×10^{26} n/m^2 (thermal) and 1.1×10^{26} n/m^2 ($E > 0.1$ MeV) at 923 K [43]

T_{test} (K)	Strain rate (min^{-1})	% Total elongation	T_{test} (K)	Strain rate (min^{-1})	% Total elongation	T_{test} (K)	Strain rate (min^{-1})	% Total elongation
823	5	5	973	5	5.5	1123	5	2
	1.2×10^{-1}	5		1.2×10^{-1}	5		1.2×10^{-1}	1
	2.4×10^{-3}	4.5		2.4×10^{-3}	4		2.4×10^{-3}	0.8
	5×10^{-6}	4		5×10^{-6}	1.5		1×10^{-6}	0.3

the JIMO mission. The calculations assumed a refractory metal alloy monolithic block core concept with an Alloy 617 pressure vessel operated for 15 years at 1 MWth. The amount of helium produced from ^{10}B was calculated with the alloy with an initial concentration of 50 wppm ($\sim$270 appm) natural boron. Helium transmutation calculations were made using the RACER Monte Carlo Reactor Physics Code [45]. The program inputs included the geometry, atomic specie, number density, neutron cross section, flux (power/time) and control position. Fig. 2 shows schematic cross sections of a pre-conceptual core geometry showing the relative locations of the outer and inner vessels.

The results show that the energy spectrum is mixed and that the flux is highly dependent on the location in the vessel, Fig. 5. Over the entire energy spectrum, the peak flux for the inner safety rod vessel (thimble) is higher than the outer vessel.

However, since the control elements are located near the outer vessel, the flux in this region contains more low energy neutrons than for the inner vessel. With operation, a change in the control element position from the beginning of life (BOL) to end of life (EOL) has a significant effect on the lower energy flux. These inhomogeneities in the energy flux distribution are responsible for variations in the production of helium. By considering the flux and neutron cross sections, the n, α reaction rates for ^{10}B and ^{58}Ni were calculated and are summarized in Fig. 6. The highest reaction rates are for ^{58}Ni because there are many more ^{58}Ni (60 wt%) atoms than ^{10}B atoms (50 wppm). Fig. 6 also shows that the reaction rate for ^{10}B increases slightly as the energy decreases, despite the lower fluxes at lower energies shown in Fig. 5. This may be explained by increases in the neutron cross section of ^{10}B as the energy decreases, which leads to higher reaction
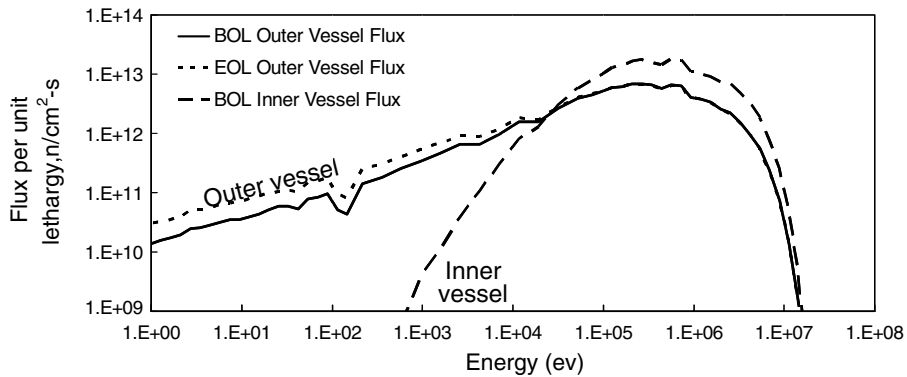

Fig. 5. The flux for the JIMO mission would have been a mixed energy spectrum that is highly dependent on the location in the vessel.
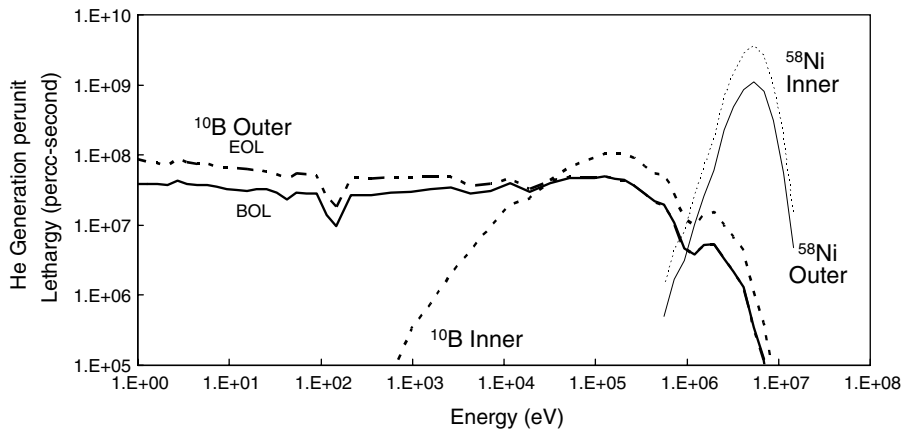

Fig. 6. The (n, α) ^{10}B reaction is a non-threshold reaction while the ^{58}Ni reaction ($^{58}Ni + n_f \rightarrow {}^{55}Fe + {}^4He$, Eq. (1)) requires a threshold energy of about 1 MeV to occur.

rates. These results illustrate the importance of analyzing the reaction rates with fine energy spectrum resolution as it would otherwise be difficult to relate helium production to fluence in the tradition sense of total thermal ($E < 0.1$ MeV) or fast neutrons ($E > 1.0$ MeV) as typically presented in the literature.

Integrating the area underneath the curves in Fig. 6 with respect to time produced the results shown in Table 8. By the end of life, the inner vessel region would be expected to produce up to ≈20 appm helium while the outer vessel region would be expected to produce up to ≈10 appm. As the boron content decreased from 50 wppm to 0 wppm, the transmuted helium was not significantly reduced for the inner vessel because most of the helium is generated from ^{58}Ni and ^{60}Ni reactions. For the middle of the outer vessel, a reduction in boron from 50 wppm to 0 wppm decreased the end of life helium from 10 appm to ∼6 appm, reflecting the almost 4 appm contribution from ^{10}B (n, α) reactions. Additional details for the helium production as a function of operational time and

isotope are shown in Figs. 7(a) and (b), for the inner vessel and outer vessel, respectively. These figures show that the production of helium from ^{58}Ni, ^{60}Ni and ^{10}B is essentially linear with time, with helium produced from the two step ^{58}Ni/^{59}Ni reaction being more parabolic, as expected. [46] This incubation period is more noticeable for the outer vessel, Fig. 7(b), due to the larger flux of thermal neutrons. Since the amount of helium produced from ^{10}B is not saturated with time, not all of the ^{10}B has been converted to ^{7}Li and ^{4}He.

Correlations between helium and the mechanical properties of Ni-base alloys are very limited as most studies have either focused on correlating helium with swelling or determining fluence and temperature effects on mechanical properties. A systematic study investigating He and mechanical properties is lacking, although 10 appm helium has been associated with the embrittlement of stainless steel alloys above 773 K [47]. The most relevant study reports results from Fe–45Ni–20Cr alloys that were either implanted with helium or irradiated with neutrons in a VVR-M reactor at 463–543 K [48]. Tensile

Table 8
The calculated amount of helium (appm) produced in Alloy 617 at four regions in a proposed JIMO reactor pressure vessel at the end of life

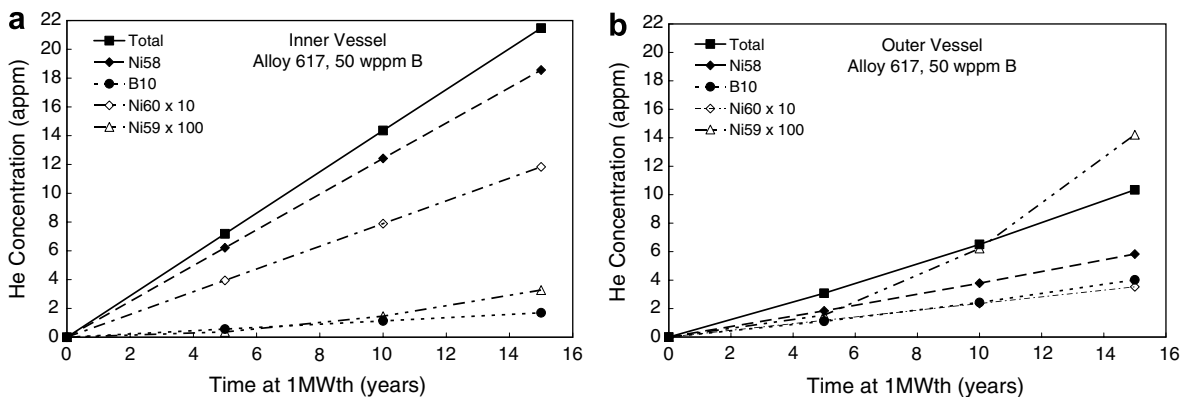| Region	Helium with 50 wppm B	Contribution % from				Helium with 0 wppm B
		^{58}Ni	^{59}Ni	^{60}Ni	^{10}B	
OD, middle	10.3	53.5	0.9	3.4	39.1	6.3
OD, bottom	1.2	59.4	0.1	3.9	33.5	0.8
ID, middle	22.4	82.0	0.2	5.4	7.5	20.7
ID, bottom	5.6	78.0	0.0	5.0	12.4	4.9

OD, outer diameter; ID, inner diameter.

Fig. 7. Calculations showing the amount of helium generated in Alloy 617 containing 50 wppm of natural boron for various isotopes as a function of operational years. (a) Inner safety rod vessel (thimble) and (b) outer vessel. The values shown for ^{59}Ni and ^{60}Ni are multiplied by 100 and 10, respectively. (a) Inner safety rod vessel (thimble) (b) outer vessel.

testing up to 923 K revealed decreases in the elongation regardless of the method for He introduction up to 6 appm. Beyond about 6 appm of helium, the uniform elongation reached a plateau of ~20% of the unirradiated elongation value. Another analysis based on early literature tensile results advocated that 2.7 wppm of natural boron or 3 appm of He was sufficient to embrittle Nimonic PE16 [49]. However, no helium measurements or microstructural characterization was conducted to justify this assertion. No studies have been able to separate the effects of helium from solute segregation, so specifying a critical level of helium that would cause embrittlement is not presently possible.

7. Mitigation of radiation-induced embrittlement

Methods to reduce the effects of irradiation on the high temperature properties of Ni-base alloys have been proposed [23] and investigated by many researchers. These approaches have included removing ^{10}B, reducing the grain size, reducing the grain boundary tensile stress, retaining He within the grains via precipitates (trapping sites), increasing the surface energy to form a void, using grain boundary precipitates to inhibit grain boundary sliding and conducting thermal mechanical treatments prior to irradiation. Examples of studies to explore these remedial methods are briefly reviewed.

Several researchers have reported a beneficial effect of lower boron on post-irradiation ductility. The most significant benefit was reported for Hastelloy X irradiated between 1 and 10×10^{24} n/m^2 (thermal) at unspecified conditions. Fig. 8 shows
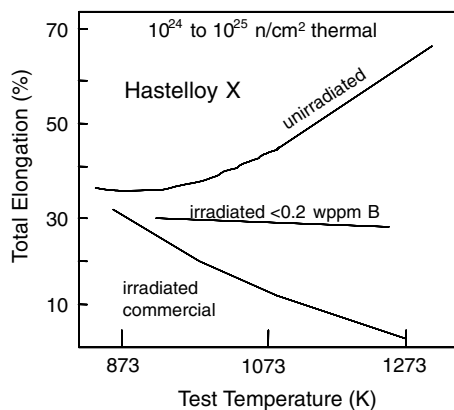
Fig. 8. An improvement in the post-irradiation tensile ductility of Hastelloy X was reported by lowering the boron content to an ultra-low level of <0.2 wppm [22].

that irradiated Hastelloy X with <0.2 wppm B displayed ~28% total elongation while commercial material, with presumably more boron, exhibited progressively less ductility as the test temperature increased [22]. In another study, only a slight benefit of 1.1 wppm B was observed over 3.8 wppm B when Hastelloy X was tensile tested at 1173 K after thermal neutron exposure of 2.4×10^{23} n/m^2 [32], suggesting low sensitivity to helium effects at these conditions. Experiments on PE16 have indicated a beneficial effect of lower boron and thermal treatment on the tensile ductility after irradiation to 20–29 dpa (4×10^{26}–5.8×10^{26} n/m^2) in the Dounreay fast reactor at 823 K [19]. Reducing the boron content from 82 wppm to 18 wppm resulted in total elongations of over 10% with heat treatment 2 as opposed to several percent with heat treatment 1, Table 9. Heat treatment 1, 1300 K for 0.3 h + 1023 K for 4 h, produced extensive amounts of intragranular carbides and 10 nm γ'. Heat treatment 2 resulted in more ductility and exhibited intragranular TiC, 30 nm γ' and grain boundaries nearly free of carbides. The mechanism responsible for these results was not reported, however, the lower level of boron in conjunction with boron trapping in the matrix by TiC, may be responsible.

The premise of boron trapping is to keep helium from reaching the grain boundaries by trapping the inert gas at high energy interfaces of matrix precipitates and to getter boron in these matrix precipitates. Analysis of Ni-base alloys after solidification and thermal mechanical processing shows that significant boron can exist at grain boundaries prior to irradiation. However, nuclear reactions will displace helium several microns from the location of the originating boron atom, delaying helium embrittlement until the helium atoms diffuse to the grain boundary. The beneficial effects of boron trapping may explain the results shown in Table 9 [19].

Table 9
The post-irradiation tensile ductility of Nimonic PE16 as a function of boron and heat treatment

Boron (wppm)	Percent elongation	
	Heat treatment 1	Heat treatment 2 grain
18	2.3	15.0
37	1.0	6.0
60	0.5	2.2
82		5.8

Neutron irradiation of 20–29 dpa (4–5.8×10^{26} n/m^2) at 823 K [19].

Some support for this remedial measure was provided by systematic experiments with Alloy 800 exposed to the mixed spectrum at Oak Ridge Reactor as a function of Ti content [50]. The authors reported that an optimized amount of Ti at 0.1 wt% exhibited the best post-irradiation creep-rupture ductility and was attributed to the retention of He within the grains at a fine dispersion of Ti-rich precipitates. However, no microscopy was reported to support these claims. In related studies on austenitic stainless steels, a fine matrix distribution of TiC or phosphides were correlated with improved mechanical properties and was attributed to helium trapping at matrix precipitates [47,51,52]. Microstructural characterization observed large bubbles for material with coarse precipitates, while almost no grain boundary bubbles were observed for materials with fine precipitates, which possessed a fine dispersion of voids at these matrix precipitates. For Ni-base alloys, oxide dispersion strengthened MA754 was proton irradiated from 723 K to 873 K after helium implantation to assess the effect of incoherent matrix–precipitate interfaces on swelling [53]. Voids were found to nucleate preferably at the oxide–matrix interface, but an expected reduction in swelling was not observed. No mechanical tests were conducted to assess embrittlement.

The effect of pre-irradiation thermal mechanical treatments was investigated for PE16 prior to exposure to 7×10^{26} n/m^2 ($E > 0.1$ MeV) [54]. Very few or no helium bubbles were observed along grain boundaries for material given a 30% cold work treatment as compared to material annealed after the 30% cold work treatment at 1073 K. Microstructural analysis did not reveal matrix TiC precipitates and additional studies were not conducted to further understand these results.

8. Recommendations for mitigating radiation-induced embrittlement of JIMO vessel

A review of the literature and design considerations revealed a concern for the use of a Ni-base alloy pressure vessel for the JIMO mission due to radiation-induced embrittlement. This embrittlement is believed to be caused by a combination of helium and second phase precipitation at grain boundaries, although a full understanding between exposure conditions and material has not been established. Despite this, the primary controlling variables are believed to be the neutron fluence, temperature, stress and alloy composition and heat treatment condition. Lower fluences are preferred and so are lower stresses at temperature. These design considerations are bounded by the properties of the currently developed commercial materials. Since nickel-base alloys were not designed for neutron exposure at elevated temperatures, the development of nuclear grade materials is warranted. Prior research has shown several promising paths for improving the embrittlement resistance through composition and thermal mechanical treatments. The removal of ^{10}B is evident as a control measure, either by reducing all boron or only ^{10}B. This could be achieved by controlling the boron content of the scrap during alloy fabrication. It is not clear how important boron is to the mechanical behavior such as the creep strength, but ^{11}B could be used exclusively to avoid helium transmutation and maintain other properties.

Materials considered for the vessel were primarily Ni-base alloys and the removal of nickel is more of an academic consideration unless cobalt-based alloys are pursued. If so, the nickel content could be reduced by approximately a factor of two to three for commercially available cobalt-based alloys, such as Alloy 188 (39Co–22Ni–22Cr–14 W). Cobalt-59 has 1/50 of the n, α reaction rate as ^{58}Ni and would produce 1/50 as much helium by the threshold reaction

$$^{59}\text{Co} + n_\text{f} \rightarrow {}^{56}\text{Mn} + {}^{4}\text{He}. \tag{5}$$
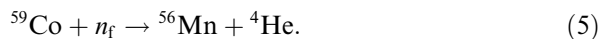
Cobalt would also eliminate helium production from the two-step ^{58}Ni, ^{59}Ni, ^{56}Fe reaction. Solute segregation can be reduced by lowering the levels of Al, Nb, Ti and Si as well as keeping metalloids very low. Examples of proposed radiation resistant Ni-base alloy compositions are shown in Table 1. The nuclear grade (NG) versions stay within the current specification while reducing elements believed to be responsible for helium embrittlement (boron) and solute segregation (Al, Si, Ti). The low (L) grade versions go beyond the current compositional specifications. Screening experiments are recommended to determine structure to property relationships with comparisons to commercially available materials. One such study was proposed, but abandoned when the program was restructured.

9. Conclusions

Radiation damage was a major concern for Ni-base structural materials considered for the JIMO

mission. A literature review and helium transmutation calculations revealed the following conclusions:

(1) Ni-base alloys are significantly embrittled after neutron exposure at elevated temperatures. This embrittlement has been attributed to a combination of helium and second phase precipitation at grain boundaries.

(3) Experimental studies are required to assess radiation-induced embrittlement under prototypical conditions.

(4) Radiation-induced swelling and creep would not be expected to exceed design allowables of 1% each.

(5) It is strongly recommended that nuclear grade Ni-base and cobalt-based alloys be pursued as a method to mitigate radiation-induced embrittlement by reducing helium generation and solute segregation.

(6) Alternative designs to the inner safety rod pressure vessel (thimble) need to be seriously pursued as the current understanding indicates that a Ni-base alloy thimble may be significantly embrittled by radiation.

Acknowledgements

References

[1] J.L. Laidler, J.J. Holmes, J.W. Bennett, in: International Conference: Radiation Effects in Breeder Reactor Structural Materials, American Institute of Mining, Metallurgical and Petroleum Engineers, 1977, p. 41.

[2] R.W. Powell, Superalloys in Fast Breeder Reactor, HEDL-SA-811, 1976.

[3] J.L. Straalsund, R.W. Powell, B.A. Chin, J. Nucl. Mater. 108&109 (1982) 299.

[4] J.F. Bates, R.W. Powell, J. Nucl. Mater. 102 (1981) 200.

[5] R. Bajaj, R.P. Shogan, C. DeFlitch, R.L. Fish, M.M. Paxton, M.L. Bleiberg, in: Proceedings of the 10th International Symposium on Effect of Radiation on Material, ASTM STP 725, 1981, p. 326.

[6] R.M. Boothby, J. Nucl. Mater. 230 (1996) 148.

[7] A.F. Rowcliffe, in: S. Zinkle, (Ed.), Critical Assessment of Structural Materials for Space Nuclear Applications, ORNL/LTR/NR-JIMO/04-08, 2005, p. 9.

[8] H. Schroeder, Radiat. Eff. 78 (1983) 297.

[9] K.F. Allbeson, C. Brown, J. Gillespie, Nucl. Eng. 31 (1) (1990) 87.

[10] Haynes 230 Alloy, Haynes High-Temperature Alloys, H-3000F, 1991.

[11] K. Natesan, A. Purohit, S.W. Tam, Materials Behavior in HTGR Environments, NUREG/CR-6824, ANL-02/37, Argonne National Laboratory, 2003, p. 19.

[12] F.A. Garner, in: B.R.T. Frost (Ed.), Materials Science and Technology, Nuclear Materials, vol. 10A, VCH, 1987, p. 420.

[13] J.I. Bramman, C. Brown, J.S. Watkins, C. Cawthorne, E.J. Fulton, P.J. Barton, E.A. Little, in: International Conference: Radiation Effects in Breeder Reactor Structural Materials, The Metallurgical Society of AIME, 1977, p. 479.

[14] J.S. Watkins, J.H. Gittus, J. Standring, in: International Conference: Radiation Effects in Breeder Reactor Structural Materials, The Metallurgical Society of AIME, 1977, p. 467.

[15] W.K. Appleby, D.W. Sandusky, U.E. Wolff, J. Nucl. Mater. 43 (1972) 213.

[16] F.A. Garner, D.S. Gelles, in: Packan and Stoller, (Eds.), Proceedings of the 14th International Symposium on Effects of Radiation on Materials. ASTM STP 1046, 2, 1990, p. 673.

[17] M.M. Paxton, B.A. Chin, E.R. Gilbert, R.E. Nygren, J. Nucl. Mater. 80 (1979) 144.

[18] A.J. McSherry, M. Patel, Results from the First Interim Examination of the Advanced Alloy Creep In-Bending Test, National Cladding/Duct Materials Development Program Quarterly Technical Progress Letter, TC-160-21, Hanford Engineering Development Laboratory, 1979, p. 3.

[19] J. Barnaby, P.J. Barton, R.M. Boothby, A.S. Fraser, G.F. Slattery, in: Proceedings of the International Conference: Radiation Effects in Breeder Reactor Structural Materials, The Metallurgical Society of AIME, 1977, p. 159.

[20] K.E. Moore, R.G. Brengle, T.G. Parker, Hastelloy X Cladding Materials Evaluation, SNAP Reactor, SNAP Program C-92b, AI-AEC-13083, 1973.

[21] K.S. Lee, Nucl. Technol. 66 (1984) 241.

[22] J.R. Lindgren, Nucl. Technol. 66 (1984) 607.

[23] D.R. Harries, J. Brit. Nucl. Energ. Soc. 5 (1966) 74.

[24] L.K. Mansur, E.H. Lee, P.J. Maziasz, A.P. Rowcliffe, J. Nucl. Mater. 141–143 (1986) 633.

[25] R.M. Boothby, J. Nucl. Mater. 186 (1992) 209.

[26] G.A. Young, R. Najafabadi, W. Strohmayer, D.G. Baldrey, W.L. Hamm, in: G.S. Was (Ed.), Proceedings of the 11th International Conference on the Environmental Degradation of Materials in Nuclear Systems, American Nuclear Society, Chicago, IL, 2003, p. 758.

[27] R.W. Smith, W.T. Geng, C.B. Geller, R. Wu, A.J. Freeman, Scr. Mater. 43 (2000) 957.

[28] H.J. Busboom, P.W. Mathay, Fast Neutron Damage Studies in High Nickel Alloys, General Electric Atomic Power report, GEAP-4985, AEC Research and Development Report, 1966.

[29] F.A. Garner, B.M. Oliver, L.R. Greenwood, J. Nucl. Mater. 258–263 (1998) 1740.

[30] L.R. Greenwood, J. Nucl. Mater. 115 (1983) 137.

[31] L.R. Greenwood, F.A. Garner, B.M. Oliver, M.L. Grossbeck, W.G. Wolfer, J. ASTM Int. Paper ID JAI11365, 1, 4 (2004) 529.

[32] K. Watanabe, Y. Ogawa, M. Kikuchi, T. Kondo, Ductility Loss of Neutron-Irradiated Hastelloy-X at Elevated Temperatures, JAERI Research Report JAERI-M 8807 (1980).

[33] T. Kondo, Development and Testing of Alloys for Primary Circuit Structures of a VHTR, Specialists' Meeting on High Temperature Metallic Materials for Application in Gas-Cooled Reactors. Vienna, Austria, IAEA, International

Working Group on Gas-Cooled Reactors, IWGGCR-4 (1981).

[34] R.M. Boothby, J. Nucl. Mater. 171 (1990) 215.

[35] D.R. Harries, J. Nucl. Mater. 82 (1979) 2.

[36] T.R. Allen, J.T. Busby, G.S. Was, E.A. Kenik, J. Nucl. Mater. 255 (1998) 44.

[37] R.A. Mulford, C.J. McMahon, D.P. Pope, H.C. Feng, Metal. Trans. A 7A (1976) 1183.

[38] P.S. Sklad, R.E. Clausing, E.E. Bloom, in: F.R. Shober (Ed.), Irradiation Effects on the Microstructure and Properties of Metals, ASTM STP, 611, American Society for Testing and Materials, Philadelphia, 1976, p. 139.

[39] W.J.S. Yang, J. Nucl. Mater. 108–109 (1982) 339.

[40] W.J.S. Yang, L.E. Thomas, D.S. Gelles, J.L. Straalsund, The Role of Solute Segregation in Postirradiation Ductility Loss, National Cladding/Duct Materials Development Program Quarterly Technical Progress Letter. TC-160-21, Hanford Engineering Development Laboratory, 1979, p. 262.

[41] W.J.S. Yang, Microstructures of Solution-Treated, Unirradiated Nimonic PE16 and Inconel 706 Duct Materials in the Ductility Trough, National Cladding/Duct Materials Development Program Quarterly Technical Progress Letter. TC-160-20, Hanford Engineering Development Laboratory, 1979, p. 187.

[42] R. Bajaj, C. DeFlitch, R.P. Shogan and M.L. Bleiberg, Special Tensile Tests on Advanced Alloys, National Cladding/Duct Materials Development Program Quarterly Technical Progress Letter, TC-160-20, Hanford Engineering Development Laboratory, 1979, p. 261.

[43] R. Bajaj, R.P. Shogan, C. DeFlitch, Special Tensile Tests on Advanced Alloys, National Cladding/Duct Materials Development Program Quarterly Technical Progress Letter. TC-160-18, Hanford Engineering Development Laboratory, 1978, p. 229.

[44] B. Bohm, K.-D. Gloss, Effects of strain rate on high temperature mechanical properties of irradiated Incoloy 800 and Hastelloy X, Radiation effects in breeder reactor structured materials, in: M.L. Bleiberg, J.W. Bennett, (Eds.), TMS, 1977, p. 347.

[45] T.M. Sutton, F.B. Brown, F.G. Bischoff, D.B. MacMillan, C.L. Ellis, J.T. Ward, C.T. Ballinger, D.J. Kelly, L. Schindler, The Physical Models and Statistical Procedures Used in the RACER Monte Carlo Code. KAPL-4840, UC-505, DOE/TIC-4500-R75, Knolls Atomic Power Laboratory, July 1999. TIS-866-3120, March 22, 2000.

[46] L.K. Mansur, A.F. Rowcliffe, M.L. Grossbeck, R.E. Stoller, J. Nucl. Mater. 139 (1986) 228.

[47] W. Kesternich, J. Nucl. Mater. 127 (1985) 153.

[48] V.F. Vinokurov, I.V. Gorynin, G.T. Zhdan, Sh.Sh. Ibragimov, O.A. Kozhevnikov, V.F. Reutov, S.A. Fabritsiev, V.D. Yaroshevich, Soviet Atom. Energ. 162 (3) (1987) 194.

[49] R.S. Barnes, Nature 206 (1965) 1307.

[50] D.G. Harman, Post Irradiation Tensile and Creep-Rupture Properties of Several Experimental Heats of Incoloy 800 at 700 and 760C, Oak Ridge National Lab, ORNL-TM-2305, 1968.

[51] E.H. Lee, A.F. Rowcliffe, E.A. Kenik, J. Nucl. Mater. 83 (1979) 79.

[52] E.H. Lee, L.K. Mansur, A mechanism of swelling suppression in phosphorous-modified Fe–Ni–Cr Alloys, J. Nucl. Mater. 141–143 (1986) 695.

[53] H. Shiraishi, A. Hasegawa, J. Nucl. Mater. 155–157 (1988) 1049.

[54] A.L. Chang and M.L. Bleiberg, Comparison of Microstructures in Neutron Irradiated Nimonic PE16 of Different Thermal Mechanical Treatments, National Cladding/Duct Materials Development Program Quarterly Progress Letter, TC-160-27, Hanford Engineering Development Laboratory, 1980, p. 199.

[55] D.J. Mazey, W. Hanks, D.E.J. Bolster, B.C. Sowden, Nucl. Energ. 28 (2) (1989) 97.

[56] F.-H. Huang, R.L. Fish, in: F.A. Garner, J.S. Perrin (Eds.), Effects of Radiation on Materials: Twelfth International Symposium, ASTM STP, 870, American Society for Testing and Materials, 1985, p. 720.

[57] Nimonic Alloy PE16, Special Metals Publication Number SMC0102, 2004, p. 19.

[58] P.C.L. Pfeil and D.R. Harries, Effects of Irradiation in Austenitic Steels and Other High-Temperature Alloys, Flow and Fracture of Metals and Alloys in Nuclear Environments. ASTM Special Technical Publication 380, ASTM, 1964, p. 202.